Hindawi
Journal of Electrical and Computer Engineering
Volume 2024, Article ID 9050909, 13 pages
https://doi.org/10.1155/2024/9050909

Research Article

Empirical Wavelet Transform Based ECG Signal Filtering Method

S. Elouaham,[1] A. Dliou,[1] W. Jenkal,[1] M. Louzazni,[2] H. Zougagh,[3] and S. Dlimi[4]

[1]*Information Systems and Technology Engineering Laboratory, National School of Applied Sciences, Ibn Zohr University, Agadir, Morocco*
[2]*Science Engineer Laboratory for Energy, National School of Applied Sciences, Chouaib Doukkali University of El Jadida, El Jadida, Morocco*
[3]*Informatic Department, Faculty of Sciences and Techniques, Sultan Moulay Slimane University, Beni Mellal, Morocco*
[4]*Information and Communication Science and Technology Laboratory, Faculty of Sciences, Chouaib Doukkali University, El Jadida, Morocco*

Correspondence should be addressed to S. Elouaham; elouaham.s@ucd.ac.ma

Received 15 September 2023; Revised 20 November 2023; Accepted 1 March 2024; Published 12 March 2024

Academic Editor: Andrea Tani

The electrocardiogram (ECG) is a diagnostic tool that provides insights into the heart's electrical activity and overall health. However, internal and external noises complicate accurate heart issue diagnosis. Noise in the ECG signal distorts and introduces artifacts, making it difficult to detect subtle abnormalities. To ensure an accurate evaluation, noise-free ECG signals are crucial. This study introduces the empirical wavelet transform (EWT), a contemporary denoising method. EWT decomposes the signal into frequency components, allowing detailed analysis by constructing a customized wavelet basis. Researchers and practitioners can enhance signal analysis by separating the desired components from unwanted noise. The EWT approach effectively eliminates noise while maintaining signal information. The study applies DWT-ADTF, FST, Kalman, Liouville–Weyl fractional compound integral filter LW, Weiner, and EWT denoising methods to two ECG databases from MIT-BIH, which encompass a wide range of cardiac signals and noise levels. The comparative analysis highlights EWT's strengths through improved signal quality and objective performance metrics. This adaptive transform proves promising for denoising ECG signals and facilitating accurate analysis in clinical and research settings.

1. Introduction

The electrocardiogram (ECG) is a widely utilized and noninvasive medical tool employed to assess the cardiac health of patients. This painless test, typically conducted in clinical settings, yields quick results. The ECG is a key diagnostic tool for determining underlying disorders as it tracks the heart's rhythm and looks for aberrant electrical activity [1]. It provides a quick and effective way to examine how the heart works and diagnoses a variety of cardiovascular conditions, including coronary heart disease, arrhythmias, and myocardial infarction. Thanks to continuous technological improvements, ECGs will remain essential for patient diagnosis and treatment, providing clinical teams with vital information about patients' health. Electrocardiography (ECG) has become indispensable for identifying cardiovascular diseases (CVDs), responsible for approximately 31% of fatalities worldwide [1, 2], due to its high accuracy and cost-effectiveness.

Advancements in technology have revolutionized the monitoring of cardiac signals, providing a deeper understanding of our heart's well-being. However, during the recording of electrocardiogram (ECG) signals, interference and unwanted artifacts can contaminate the data. This occurs when external sources or patient movement introduces electrical noise, which is then captured by the electrodes used for data acquisition, resulting in distorted ECG tracings. The presence of such noise can lead to misinterpretation and hinder accurate diagnosis, as it distorts waveform patterns and compromises the reliability of ECG readings. Common types of noise in ECG signals include power-line interference, motion artifacts, electrode interface

issues, poor electrode-skin contact, and white Gaussian noise, all of which introduce high-frequency components that interfere with signal interpretation [3–9].

To address this challenge, employing proper filtering techniques becomes essential for reducing noise and obtaining reliable ECG signals. Filtering the ECG signals can unveil vital information about the heart, enabling early diagnosis, improved risk assessment, and more effective treatments for cardiovascular diseases. Filtering plays a crucial role in the interpretation process by eliminating noise and artifacts that can affect the accurate analysis of important features such as the PQRST waves. It also facilitates the isolation of signals at different frequencies, enabling comprehensive study and analysis. When performed correctly, filtering ECG signals empowers clinicians to make more precise diagnoses of cardiovascular conditions and diseases, thereby enhancing patient care and outcomes. Recognizing the significance of filtering ECG signals allows us to take proactive measures in safeguarding ourselves against this life-threatening condition.

Numerous techniques have been extensively studied in the scientific literature to tackle the issue of noise in ECG signals, reflecting the ongoing efforts to improve signal quality. Empirical mode decomposition (EMD) and its variants have emerged as popular choices [10–17], offering a data-driven approach that adaptively decomposes the signal into intrinsic mode functions. Discrete wavelet transform (DWT) has also gained significant attention [17–22], enabling a multiresolution analysis of the signal by decomposing it into different frequency bands. Adaptive filtering techniques [21, 22] provide adaptability to varying noise conditions, allowing for a real-time noise cancellation by dynamically adjusting filter parameters.

Other notable approaches include Weiner and Kalman denoising techniques [23, 24], which utilize statistical estimation to remove noise from the ECG signal. The Liouville–Weyl filter [25] addresses noise removal through a combination of time and frequency domain processing, thereby incorporating the strengths of both domains. The fractional Stockwell transform (FST) [26] represents a novel method that combines wavelet decomposition and short-time Fourier transform to achieve enhanced denoising capabilities.

While these methods exhibit promise in mitigating noise in ECG signals, it is important to note that each approach has its own set of advantages and disadvantages. Factors such as computational complexity, adaptability to different noise types and levels, preservation of signal features, and robustness against artifacts and disturbances all contribute to the distinct characteristics of these techniques. To comprehend the trade-offs and determine the best strategy for certain applications, more research and comparison studies are required, paving the way for continued improvements in ECG signal denoising approaches.

We used the empirical mode decomposition (EMD) method, which breaks the signal down into a collection of intrinsic mode functions (IMFs), to solve the problem of noise in the signal. These IMFs are functions characterized by an equal number of extrema and zero-crossings, and their envelopes are defined by the local maxima and minima, exhibiting symmetry around zero. However, it is observed that the noise components tend to be distributed across several low-order IMFs, making their removal necessary for noise reduction.

In our denoising process, we selectively removed these IMFs containing noise constituents. While this step successfully reduced the noise, it came at the cost of losing some important information, leading to a potential drawback in signal reconstruction. Mode mixing, another challenge encountered in this process, further complicated the reconstruction of the original signal [10–12]. The phenomenon of mode mixing occurs when the different IMFs interact with each other, resulting in a distorted representation of the underlying signal.

It is important to acknowledge that the removal of specific IMFs for noise reduction is a trade-off between preserving signal fidelity and reducing unwanted noise. Striking the right balance is crucial to ensure accurate signal reconstruction while effectively suppressing noise interference. Further research and exploration of alternative methods are necessary to address the issues related to information loss and mode mixing, allowing for more robust and reliable denoising techniques in the analysis of ECG signals.

The DWT method, employing soft and hard thresholding techniques, is commonly used for noise removal in nonstationary signals. However, this method struggles to preserve edges effectively, leading to the potential loss of important signal details [16, 17]. On the other hand, the EMD-based method has shown better results compared to wavelet-based thresholding, but it may not entirely eliminate interferences.

To enhance the denoising capabilities, researchers have combined EMD and other methods with the Wavelet approach. However, this approach's major drawback lies in the challenging task of selecting the appropriate wavelet and threshold type. It requires careful consideration to achieve optimal results [26].

Adaptive filters offer an alternative approach by utilizing a reference signal closely correlated to the original signal. While this method can effectively remove noise, it is not suitable for real-time applications due to the need for a reference signal [27, 28].

In some studies, windowing techniques have been applied to preserve the QRS complex, the most crucial component of the ECG signal. However, this approach still results in residual noise in the QRS region [11]. Other research efforts have employed a combination of DWT and the adaptive double-threshold filter (ADTF) for noise removal. The DWT-ADTF hybrid approach combines the advantages of both the DWT and the ADTF methods to improve ECG signal filtering. This approach aims to handle electromyogram (EMG) noises, power-line frequency interference (50 Hz), and high-frequency noises that may interfere with the ECG signal [14]. Unfortunately, this method discards the original subband obtained from the wavelet decomposition, leading to the loss of information in higher-frequency components. One major limitation in previous works is the lack of consideration for the dynamic behavior of the ECG signal.

Weiner and Kalman filters are known for their efficiency in preserving signal edges. However, they are prone to blurring phenomena due to the integral-based blurring models utilized [23, 24]. As a result, there is a significant loss of high-frequency information in the original signal stream [29].

These limitations and challenges highlight the need for further research and development of denoising methods that can effectively address the preservation of signal details, adapt to dynamic ECG characteristics, and minimize information loss in higher-frequency components.

In a study conducted by the authors of [25], the limitations of LW (Liouville–Weyl) filters were identified. Due to their computational complexity, these filters might be difficult to use with big datasets or high-resolution signals. Furthermore, the linearity and stationarity assumptions made by the LW technique might not always hold true in real-world situations. As a result, these methods may not exhibit optimal performance when applied to denoise nonlinear and nonstationary signals.

Another research effort [26] focused on the FST (fractional Stockwell transform) denoising method. However, this method proved to be sensitive to the selection of parameters. Choosing the fractional order and threshold value for denoising requires careful consideration, as selecting incorrect parameters can lead to subpar denoising performance. It is crucial to strike the right balance and make appropriate parameter choices to achieve effective noise reduction using the FST method.

These findings highlight the importance of considering the computational complexity, linearity, stationarity, and parameter selection when utilizing LW and FST methods for denoising tasks. Future research should explore alternative approaches that can overcome these limitations and provide robust denoising performance for various types of signals, including nonlinear and nonstationary ones. By addressing these challenges, researchers can advance the development of more efficient and accurate denoising techniques in the field of signal processing.

To mitigate the impact of noise from various sources, the utilization of appropriate signal processing techniques becomes crucial. In this regard, the empirical wavelet transform (EWT) approaches [30, 31] have emerged as effective solutions. This method combines the ideas of wavelet transform (WT), empirical mode decomposition (EMD), and Fourier transform to decompose signals into their constituents at different scales. The EWT method is rooted in the empirical analysis of signals, enabling it to capture the nonstationary and nonlinear characteristics of the signal. This approach has been successfully employed in diverse fields, including the detection of bearing faults [32] in various applications such as high-speed trains [33], hydraulic pumps [34], renewable energy systems [35], and biomedical signals [36, 37]. These applications have demonstrated the favorable outcomes achieved through the implementation of the EWT method.

However, it is worth noting that the potential and performance of the EWT approach have not been directly compared with the aforementioned methods. To ascertain the effectiveness of the EWT method, a comprehensive evaluation was conducted using arrhythmia data sourced from the MIT-BIH database [38]. This evaluation encompassed various types of real-world data as well as simulated noise scenarios to thoroughly assess the suggested method's capabilities. By subjecting the EWT approach to rigorous testing and comparison, researchers aimed to establish its efficacy in denoising ECG signals and highlight its potential benefits over existing techniques. EWT is inherently adaptive and flexible. It allows the decomposition of signals into modes with varying frequency content, providing adaptability to the diverse and dynamic nature of ECG signals. It improves the segmentation of the spectra, which is crucial for identifying various disturbances in ECG signals. EWT constructs a customized wavelet basis for each signal, allowing for a tailored approach to signal analysis. This customization is particularly beneficial when dealing with ECG signals that may have unique characteristics and structures. EWT excels in frequency localization. By decomposing the signal into modes with well-localized frequencies, EWT facilitates a detailed analysis of different components of the ECG signal, helping in the separation of desired components from the unwanted noise.

The findings from this investigation will contribute to expanding the knowledge and understanding of the EWT method's capabilities, enabling researchers and practitioners to make informed decisions regarding its implementation in ECG signal processing. This approach is compared with the discrete wavelet transform with adaptive dual-threshold filtering (DWT-ADTF) technique, and the results show that our method outperforms the DWT-ADTF technique in terms of signal-to-noise ratio (SNR) and root mean square error (RMSE), and it allows for an excellent recovery of the original ECG morphology and features, making it easier to detect subtle abnormalities in the heart's electrical activity. The comparative analysis will shed light on the strengths and advantages of the EWT approach, ultimately facilitating the development of improved denoising techniques in the field of signal processing.

The structure of the paper is as follows. The Methods section provides a comprehensive overview of the theoretical principles underlying the empirical wavelet transform (EWT) and DWT-ADTF technique. In addition, this section outlines the materials utilized and presents the proposed algorithm. In order to assess the performance of the algorithm, a series of simulations were conducted, and the results are detailed in the subsequent section.

The Results section not only quantifies but also qualitatively evaluates the effectiveness of the proposed algorithm. Through these simulations, the performance of the algorithm is thoroughly analyzed, taking into account various metrics and criteria. The obtained results are then discussed and interpreted in the following section. The goal of this discussion is to give readers a greater understanding of the simulation results, as well as the algorithm's advantages, disadvantages, and room for development.

The "Conclusion" section outlines the most important conclusions and learnings from this research. The conclusions draw upon the presented simulations and discussions,

offering a comprehensive overview of the algorithm's performance and its implications. The conclusion section serves as a concise summary, encapsulating the main takeaways of the research and highlighting the contributions and significance of the proposed approach in the context of ECG signal processing.

2. Denoising Methods: Empirical Wavelet Transform

The EWT is a technique used to decompose signals into their constituents at different scales, and this method was first introduced by the authors of [30] in 2013. It combines the ideas of WT, EMD, and the Fourier transform, allowing the signal to be decomposed into a mode series. Based on the EWT analysis, the decomposition result is dependent on the spectrum segmentation. Therefore, the improvement in the segmentation of the spectra is crucial for the identification of various disturbances. It applies an adaptive filter that can be tuned according to the signal of interest and produces more accurate representations than traditional transform techniques, such as Fourier or wavelets [30–35]. As its name implies, this method relies on empirical data instead of predefined functions to produce its results. This allows for improved flexibility in analyzing a wide variety of signals with minimal computational effort and complexity. The EWT method assumes that the Fourier spectrum of the AM-FM component has a good stability [30–35]. The bandpass filter set construction can be employed to segment and filtrate the spectra, and the signal can be decomposed adaptively via several modes.

The EWT technique is described in the following steps:

(1) We first determine the spectrum $X(\omega)$ of $x(t)$ by FFT. The frequency spectrum is standardized in the interval of $[0, \pi]$. Then, we locate the local maxima in the $X(\omega)$ with their associated frequencies, and we denote them as local peak frequencies. Assuming that $X(\omega)$ is composed of N local maxima with corresponding local peak frequencies $\Omega_j, j = 1, 2, \ldots\ldots\ldots, N$, we order the detected maxima in descending order of frequency according to the amplitude of the local maxima [31, 32].

(2) On the base of the frequency dominant points of $X(\omega)$, the border $\omega = \omega_i\}i = 1, 2, \cdots, N$ of $X(\omega)$ can be found by various techniques. The manner of segmenting the specter is shown in Figure 1, and N continued intervals $\Lambda_n = [\omega_{n-1}, \omega_n]$ are obtained, where $2\tau_n$ is the transitional part of each ω_n border (represented in the green region of Figure 2) and $n \in [1, \mathrm{N}]$ and $\omega_0 = 0, \omega_{\mathrm{K}} = \pi, \tau_{\mathrm{k}} = \gamma\omega_n$.

$$\omega_n = \begin{cases} 0 \longrightarrow (n = 0), \\ \operatorname{argmin} X(\omega) \quad \longrightarrow 1 \le n \le N - 1, \Omega_{n-1} \le \omega \le \Omega_n, \\ \pi. \end{cases} \tag{1}$$

(3) Having identified the segment, the empirical scaling function $\Upsilon_1(\omega)$ and the empirical wavelet function $\mathrm{H}_n(\omega)$ can be built by the Littlewood–Paley and Meyer wavelets. Furthermore, their frequency domain forms are $\Upsilon_1(\omega)$ and respectful.

$$\Upsilon_1(\omega) = \begin{cases} 1 \cdots\cdots\cdots\cdots\cdots\cdots\cdots |\omega| \le \omega_1 - \tau_1, \\ \cos\left[\frac{\pi}{2}\beta\left(\frac{1}{2\tau_1}\left(|\omega| - \omega_1 + \tau_1\right)\right)\right] \cdots\cdots\cdots\cdots \omega_1 - \tau_1 \le |\omega|\big| \le \omega_1 + \tau_1\big|, \\ 0 \cdots\cdots\cdots\cdots\cdots\cdots\cdots \text{others}, \end{cases} \tag{2}$$

$$\mathrm{H}_n(\omega) = \begin{cases} 1 \cdots\cdots\cdots\cdots\cdots\cdots\cdots\cdots \omega_n + \tau_n \le \omega \le \omega_{n+1} - \tau_{n+1}, \\ \cos\left[\frac{\pi}{2}\beta\left(\frac{1}{2\tau_{n+1}}\left(|\omega| - \omega_{n+1} + \tau_{n+1}\right)\right)\right] \cdots\cdots\cdots \omega_{n+1} - \tau_{n+1} \le |\omega| \le \omega_{n+1} + \tau_{n+1}, \\ \sin\left[\frac{\pi}{2}\beta\left(\frac{1}{2\tau_n}\left(|\omega| - \omega_n + \tau_n\right)\right)\right] \cdots\cdots\cdots\cdots\cdots \omega_n - \tau_n \le |\omega| \le \omega_n + \tau_n, \\ 0 \cdots\cdots\cdots\cdots\cdots\cdots\cdots \text{others}, \end{cases} \tag{3}$$

where $\tau_n = \gamma\omega_n$ valid argument should be larger than zero and sufficiently small, while $\beta(x)$ represents a transition function as defined in reference [27], and this function is given by the following equation $\beta(x) = x^4(35 - 84x + 70x^2 - 20x^2)$.

(4) The number of levels of decomposition is dependent on the number of dominating frequency points, and the approximation coefficients and detail coefficients are available by empirical wavelets with low awareness.

$$W_f^{\varepsilon}(0,t) = \langle f, \Upsilon \rangle = \int f(\tau)\overline{\Upsilon_1(\tau - t)}\mathrm{d}\tau. \quad (4)$$

The detail coefficients are as follows:

$$W_f^{\varepsilon}(n,t) = \langle f, \mathrm{H}_n \rangle = \int f(\tau)\overline{\mathrm{H}_n(\tau - t)}\mathrm{d}\tau, \quad (5)$$

where <, > denotes the internal product. The exponent - denotes the conjugate of the variables.

(5) Lastly, the mode components of $u(t)$ may be generated as in equation (6), which shall be organized as a function of the frequency.

$$\begin{cases} f_0(t) = W_f^{\varepsilon}(0,t) * \Upsilon_1(t), \\ f_n(t) = W_f^{\varepsilon}(n,t) * \Psi_n(t), \end{cases} \quad (6)$$

where $*$ is the convolution calculation.

The purpose of the analytic benefit of the EWT is to be able to recognize the different distribution of signal components from spectral information and to build an adaptive filter bank that is suitable for the extraction of modes at different frequencies. The dominating point of frequency is the values of the frequencies of the various components of the signal target, which is the significant information implied in the first phase of the EWT [36].

The procedure for eliminating noise from ECG signals includes the steps outlined in this section, as depicted in Figure 2.

3. Physiology Signals

In this section, different ECG denoising methods, including DWT-ADTF, FST, Kalman, LW, Weiner, and EWT, are performed on the two ECG databases. The two ECG databases employed in this study are the MIT-BIH arrhythmia and noise stress test databases. These databases are available to the public in [39]. A short overview of these databases is presented in the following:

(1) *MIT-BIH Arrhythmia Database*. It includes a group of 48 samples taken from 47 persons, where two records were obtained from the same person, and each sample had a length of 30 minutes. These records have a sampling frequency of 360 Hz and are digitized by using an 11-bit resolution over a 10 mV range [40].

(2) *MIT-BIH Sound Stress Test Database*. It comprises a total of 15 records, 12 of which are ECG recordings of half an hour and the other 3 are typical noises, i.e., baseline drift, muscle noise (EMG), and electrode movement artifact. These noises are taken from the records by choosing their range, which is affected by the noise [40].

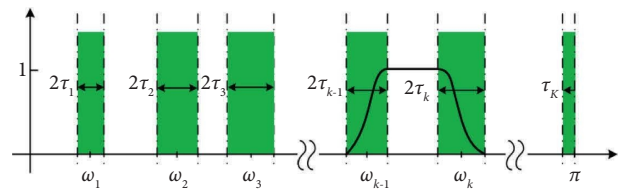

Figure 1: The spectrum segmentation basis of EWT.

The ECG signal is considered nonlinear and nonstationary. This means that the shape of an ECG waveform (its morphology) can change depending on several factors such as heart rate, level of physical activity, age, or gender; furthermore, this variability makes it difficult to make general assumptions about how any given cycle should look like. The most common source of noise that can attack ECG signals is power-line interference (PLI). PLI is a type of electromagnetic disturbance that can affect the signals in electronic devices located near the power lines. PLI occurs when electrical energy from an adjacent cable radiates or couples onto another device and interferes with its normal operation. Motion artifact (MA) is an electrical disturbance created when a patient or subject moves during the recording of electrocardiographic (ECG) signals. This kind of interference can be especially detrimental to data acquisition as it masks important features in the signal, and thus, misinterpretations can result from this type of noise. The baseline wander (BW) is an undesired drift of the baseline value in ECG recordings. This happens when there are sudden changes or shifts in electrical potentials that cause fluctuations and disruptions in signal waveforms over time. Muscle artifacts are electrical disturbances caused by muscle movements that interfere with the quality of ECG tracings during data acquisition. These types of interferences can significantly impact accurate diagnostics as they tend to mask or distort important features in waveforms such as PQRST complexes due to their amplitude and frequency. This may result in delayed potential diagnoses if they are not properly filtered out before or during analysis.

The denoising performance of the suggested method in comparison to the techniques cited above is evaluated for certain parameters such as $\mathrm{SNR_{out}}$, $\mathrm{SNR_{imp}}$, MSE, PRD, and RMSE.

The MSE is generally computed to verify the difference between the original and denoised signals. This is given in the following formula:

$$\mathrm{MSE} = \frac{1}{k}\sum_{i=1}^{k}(z(i) - \overline{z}(i))^2. \quad (7)$$

RMSE is generally computed to verify the difference between the original and denoised signals. This is given in the formula as follows:

$$\mathrm{RMSE} = \sqrt{\frac{1}{k}\sum_{i=1}^{K}(z(i) - \overline{z}(i))^2}. \quad (8)$$

PRD is computed to verify the distortion of the denoised signal with the original signal and is provided by the following formula:

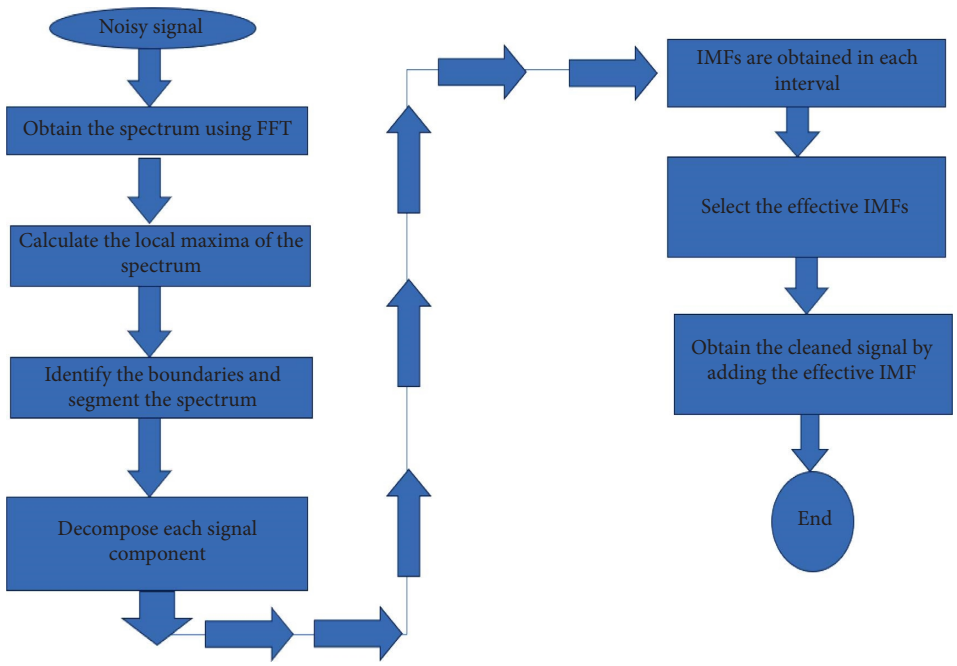

Figure 2: Flow diagram of the EWT method.

$$\mathrm{PRD} = \sqrt{\frac{(1/k)\sum_{i=1}^{K}(x(i)-\overline{x}(i))^2}{\sum_{i=1}^{K}x^2(i)}} * 100. \quad (9)$$

Here, $z(n)$ is the ECG signal before adding noise and $\overline{z}(n)$ is the reconstructed signal after filtering.

The $\mathrm{SNR_{Out}}$ equation is obtained by using the following equation:

$$\mathrm{SNR_{out}}(\mathrm{d}B) = 10 * \log_{10}\left(\frac{\sum_{i=1}^{K}[x(i)]^2}{\sum_{i=1}^{K}[x(i)-\overline{x}(i)]^2}\right). \quad (10)$$

Let $z(n)$ represent the original ECG signal before noise addition, $\overline{z}(n)$ denote the results after denoising the ECG signals, and N indicate the total number of biomedical signals utilized.

The SNR improvement, or signal-to-noise ratio improvement, is a measure of how much better a signal is compared to the noise that is present in the environment. The $\mathrm{SNR_{imp}}$ equation is given in the following equation:

$$\mathrm{SNR_{imp}}(\mathrm{d}B) = 10 * \log_{10}\left(\frac{\sum_{i=i}^{K}[z(i)-z_a(i)]^2}{\sum_{i=1}^{K}[z(i)-\overline{z}(i)]^2}\right), \quad (11)$$

where z_a is the noisy signal.

It is a measure of the signal strength relative to the noise level, and the higher the SNR improvement, the better the signal quality.

4. Experiment and Analysis

This section looks into how the EWT performs under various contaminations. The suggested algorithm is applied to the ECG signal taken from the MIT-BIH database, and this signal 115 is obtained from the PhysioNet dataset. The signal lines transporting the ECG signal from a patient to the viewing equipment are affected by electromagnetic disturbances from the 50/60 Hz power line noise that can be simulated as sinusoids [18]. This sinusoid model of the 50 Hz power line is given as

$$\mathbf{N}(\mathbf{t}) = \mathbf{A} \times \mathbf{sin}(\mathbf{2} \times \boldsymbol{\pi} \times \mathbf{f} \times \mathbf{t}), \quad (12)$$

where f is the power line frequency, A is the amplitude, and $N(t)$ is the noise on the power lines. The peak-to-peak amplitude is the noise level. The power line has a 50 Hz frequency and $A = 0.15$ mV. Similar to how power-line interference was modeled in the previous equation, this one does as well.

4.1. Qualitative Results. As an important step in the evaluation of the ECG denoising approach, the qualitative analysis of the results allows a significant study of the performances of an approach. This is due to the analysis of the distortion recovery quality of this approach.

Figure 2 shows a case of the ECG signal denoising using the proposed method. The subject signal is the MIT-BIH record 119, and the additive noise is the synthetic power-line signal. Figure 3(a) presents the original signal of 119, Figure 3(b) presents the original signal with the interfered noise of the synthetic power-line signal, and Figure 3(c) presents the reconstructed signal.

As shown in this figure, the proposed method allows an excellent recovery of the original ECG morphology and features. This is a result of the effective combination of discrete wavelet transform (DWT) and fast Fourier transform (FFT), which enables a robust performance in pinpointing the unwanted noise spectrum and removing it at the appropriate decomposition level. By integrating

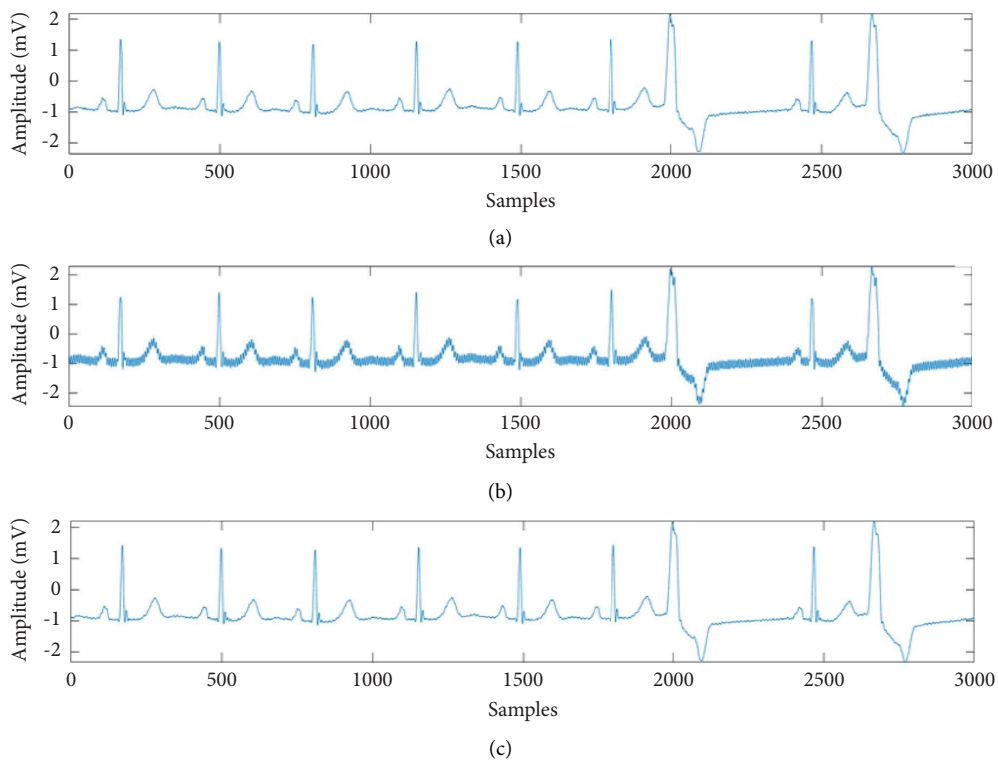

Figure 3: The denoising outcomes of the PLI, including the original signal (119) (a), the infected signal (b), and the reconstructed signal (c).

DWT and FFT techniques, we have achieved a high level of accuracy in identifying where the undesirable noise is present within the signal and removing it at the most suitable stage of signal decomposition. This synergy between DWT and FFT allows us to precisely isolate and eliminate the noise, enhancing the overall performance of the process.

Figure 3 presents a case of the ECG denoising of 15 dB SNR level of the white Gaussian noise WGN based on the proposed method. The analyzed signal, in this case, is the MIT-BIH record 103. Figure 4(a) presents the original signal of 103, Figure 4(b) presents the original signal interfered with the Gaussian noise signal, and Figure 4(c) presents the reconstructed signal.

This figure allows observing the correct reconstruction of the original ECG features as the QRS complex and the other amplitude waves. Based on these results, the proposed method shows interesting performances in terms of qualitative results, which are illustrated in Figures 3 and 4.

4.2. Quantitate Results. The results presented in Table 1 showcase the performance of the proposed method in correcting power-line interference in MIT-BIH record 115, characterized by noise $N(t)$ with an amplitude (A) of 0.15 mV and a frequency (f) of 50 Hz. The comparison includes several recent methods, namely, RL, AZP, FZP, and ADTF-DWT, as documented in [18].

The signal-to-noise ratio (SNR) is a crucial metric indicating the quality of the corrected signal. A higher SNR_{out} value signifies a better ability to recover the original signal from noise. The proposed method outperforms all other methods (RL: 6.54/AZP: 12.17/FZP: 14.25/ADTF-DWT: 23.29/proposed method: 27.6265), including the competitive ADTF-DWT approach, demonstrating its effectiveness in mitigating power-line interference, and preserving signal integrity.

The mean squared error provides a quantitative measure of the difference between the corrected signal and the true signal. A lower MSE indicates a closer match to the original signal. The proposed method achieves the smallest MSE among all methods (RL: 0.0754/AZP: 0.0206/FZP: 0.0128/ADTF-DWT: 0.0015/proposed method: 0.0007), emphasizing its accuracy in minimizing the deviation from the true signal.

Table 2 presents a comprehensive comparison between the proposed method and Liouville–Weyl filtering (LW) in the context of denoising ECG signal record 122. The simulated sinusoid's amplitude is varied across three levels ($A = 0.3$ mV, $A = 0.35$ mV, and $A = 0.4$ mV). The results highlight the efficacy of the suggested approach in comparison to the LW filtering method.

The SNR_{out} values demonstrate the superiority of the proposed method over LW filtering at each level of simulated noise amplitude ($A = 0.3$ mV: proposed method-$= 16.2537$, LW $= 14.1929$/$A = 0.35$ mV: proposed method $= 14.6951$, LW $= 13.9977$/$A = 0.4$ mV: proposed method $= 14.6312$, LW $= 13.8038$). Higher SNR_{out} values

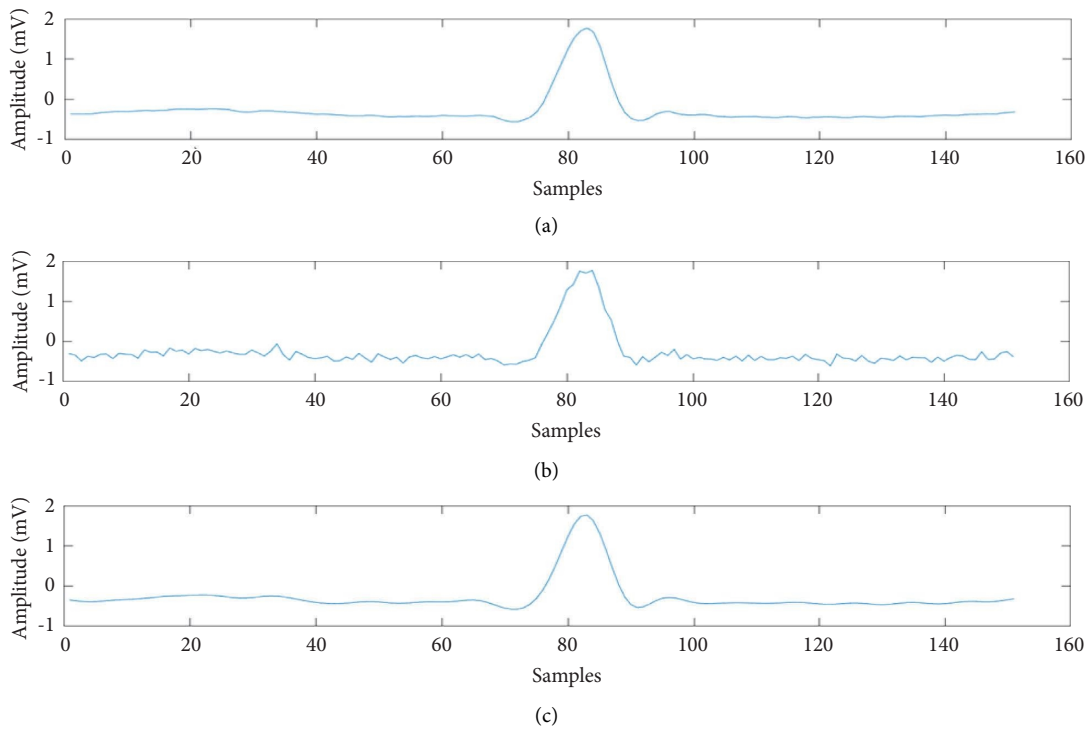

Figure 4: The results of the WGN's 15 dB of denoising: the original signal (103) (a), the infected signal (b), and the reconstructed signal (c).

Table 1: Results of the comparison of different filtering techniques.

	RL	AZP	FZP	ADTF-DWT	Proposed method
SNR_{out}	6.54	12.17	14.25	23.29	27.6265
MSE	0.0754	0.0206	0.0128	0.0015	0.0007

Table 2: Results of the comparison of different filtering techniques (EWT and LW).

		$A = 0.3$	$A = 0.35$	$A = 0.4$
SNR_{out}	Proposed method	16.2537	14.6951	14.6312
	LW	14.1929	13.9977	13.8038
MSE	Proposed method	0.0201	0.0288	0.0292
	LW	0.0235	0.0344	0.0405

signify better noise reduction and improved signal quality. The proposed method consistently outperforms LW, indicating its robustness across different noise levels.

The MSE values further support the effectiveness of the proposed method, consistently exhibiting lower error than LW filtering ($A = 0.3$ mV: proposed method = 0.0201, LW = 0.0235/$A = 0.35$ mV: proposed method = 0.0288, LW = 0.0344/$A = 0.4$ mV: proposed method = 0.0292/ LW = 0.0405). Lower MSE values indicate a closer match to the true signal, emphasizing the proposed method's accuracy in denoising ECG signals under varying noise amplitudes.

Table 3 provides a comprehensive comparison between the proposed method and two well-known denoising filters, namely, Weiner and Kalman filters, applied to the ECG signal records 103, 105, and 121. These signals are affected by both power-line interference and muscle artifact (MA), with a simulated sinusoidal interference of amplitude $A = 0.15$ mV. The results highlight the robustness of the proposed approach, which consistently outperforms the compared filters even in the presence of more complex noises.

The proposed method consistently demonstrates significantly higher SNR_{out} values than Weiner and Kalman filters, indicating superior noise reduction and preservation of signal quality in the presence of power-line interference.

The proposed method consistently yields lower MSE and PRD values than Weiner and Kalman filters for all three records.

Table 3: Results of the comparison of different filtering techniques (EWT, Weiner, and Kalman).

Noises	Filters	SNR_{out}			MSE			PRD		
		103	105	121	103	105	121	103	105	121
Power-line interference	Proposed method	**28.9456**	**30.4729**	**37.0877**	**0.00019**	**0.00014**	**0.0002**	**3.5704**	**2.9947**	**1.3984**
	Weiner	6.9821	6.4314	9.2382	0.0741	0.1255	0.048	57.026	61.694	39.436
	Kalman	4.766	5.4244	6.4117	0.1510	0.1434	0.1242	80.89	69.733	60.531
MA	Weiner	6.9001	5.3253	8.9682	0.0683	0.1971	0.0492	56.615	74.624	40.452
	Kalman	5.3188	5.2970	7.4177	0.1292	0.1863	0.0929	74.109	74.152	52.178
	Proposed method	**7.7482**	**8.1272**	**16.3303**	**0.0253**	**0.0241**	**0.0240**	**40.9818**	**39.2319**	**15.2576**

The proposed method give the good results.

Table 4: Results of the comparison of different filtering techniques (RL, AZP, FZP, and ADTF-DWT).

	RL	AZP	FZP	ADTF-DWT	Proposed method
SNR_{out}	6.38	11.82	13.68	15.69	18.1048
MSE	0.0705	0.0223	0.0146	0.0069	0.0064

The proposed method outperforms Weiner and Kalman filters in denoising MA interference, as evidenced by higher SNR_{out} and lower MSE and PRD values for all three records. This suggests that the proposed method is more effective in handling complex noise scenarios associated with muscular activity during ECG signal recording.

Table 4 presents the results of the denoising process applied to signal 115 from the MIT-BIH database, focusing on EMG interferences. The comparison includes various denoising filters, specifically RL, AZP, FZP, ADTF-DWT, and the proposed method. The evaluation metrics, SNR_{out} and MSE, provide insights into the performance of each method in reducing the impact of EMG interferences on the signal.

The SNR_{out} values reveal that the proposed method achieves a significantly higher signal quality than the other denoising filters. A higher SNR_{out} indicates a better noise reduction and improved fidelity of the signal. The proposed method outperforms RL, AZP, FZP, and ADTF-DWT, thereby reinforcing its effectiveness in handling EMG interferences.

The MSE values further emphasize the superior performance of the proposed method. Lower MSE values indicate a closer match between the denoised signal and the true signal. The proposed method achieves the lowest MSE among all compared filters, highlighting its accuracy in preserving signal details.

Table 5 presents compelling findings from an investigation focused on comparing the hybridization of adaptive dual-threshold filtering (ADTF) and discrete wavelet transform (DWT) applied to various signals extracted from the Arrhythmia dataset. The study specifically introduces additive white Gaussian noise (WGN) at a signal-to-noise ratio (SNR) level of 5 dB. The evaluation metrics employed for this comparative analysis include mean squared error (MSE), root mean squared error (RMSE), percentage residual difference (PRD), and signal-to-noise ratio improvement (SNR_{imp}). The results demonstrate the promising performance of the proposed method, leveraging multidecomposition levels of analysis through both DWT and empirical mode decomposition (EMD) approaches. The hybridization of ADTF and DWT, when applied to signals affected by additive WGN, exhibits favorable outcomes based on the specified evaluation metrics. These findings underscore the potential efficacy of the proposed method in enhancing the denoising process and preserving signal integrity in the presence of simulated noise conditions.

Table 6 provides a comparative analysis of several denoising filters, namely, Stockwell transform (ST), fractional Stockwell transform (FST), and the proposed method, applied to correct muscular artifact (MA) interferences in signal 222 from the MIT-BIH database. The evaluation metrics include the mean squared error (MSE) and root mean squared error (RMSE) [26, 30].

The results for MA interference denoising demonstrate the superior performance of the proposed method compared to FST and ST. The significantly lower MSE and RMSE values for the proposed method suggest that it is more effective in preserving the original signal while reducing the impact of muscular artifacts. This indicates that the proposed method outperforms both FST and ST in terms of accuracy and fidelity in MA interference correction.

Similarly, for electrode motion (EM) interference denoising, the proposed method exhibits competitive performance. While FST achieves an impressively low MSE and RMSE, the proposed method maintains a good balance between accuracy and robustness. ST, on the other hand, has higher MSE and RMSE values, indicating comparatively less effectiveness in handling EM interference.

Table 7 showcases the denoising performance of three filtering techniques, namely, empirical mode decomposition (EMD) with white Gaussian noise added (EWT), ensemble empirical mode decomposition (EEMD), and complete ensemble empirical mode decomposition with adaptive noise (CEEMDAN). The evaluation metrics include mean squared error (MSE), root mean squared error (RMSE), and percentage residual difference (PRD) for various signal-to-noise ratio (SNR) levels [41].

The table presents the signal-to-noise ratio improvement (SNR_{imp}) for the three denoising methods (EEMD, CEEMDAN, and EWT) across different SNR levels.

Table 5: The results of the proposed method for denoising artificial interferences (WGN of 5 dB) in certain signals from the MIT-BIH database.

	MSE		RMSE		PRD		SNR_{imp}	
	Proposed method	ADTF-DWT	Proposed method	ADTF-DWT	Proposed method	ADTF-DWT	Proposed method	ADTF-DWT
222	0.0022	0.0023	0.0469	0.0479	23.8600	24.6113	7.4466	7.3829
123	0.0337	0.0360	0.1836	0.1897	20.7093	20.8566	8.6767	8.6498
122	0.0277	0.0411	0.1663	0.202	18.0512	22.75	9.8699	8.07
119	0.0430	0.0459	0.2074	0.214	20.8363	21.92	8.6236	8.13
117	0.0261	0.0283	0.1616	0.168	19.1211	19.18	9.3698	9.34
105	0.0061	0.0062	0.0786	0.0787	19.8824	20.56	9.0306	8.6873

Table 6: Results of the comparison of different filtering techniques (ST, FST, and proposed method).

		MSE	RMSE
MA	Proposed method	**0.0240**	**0.1550**
	FST	0.0439	0.2097
	ST	1.5275	1.2066
EM: ELECTROD Motion	Proposed method	0.0440	0.210
	FST	**0.003**	**0.0616**
	ST	0.036	0.1895

The bold signified the good results.

Table 7: Results of the comparison of different filtering techniques (EEMD, CEEMDAN, and EWT).

SNR (dB)	EWT			EEMD			CEEMDAN		
	MSE	RMSE	PRD	MSE	RMSE	PRD	MSE	RMSE	PRD
−10.0000	0.4262	0.6528	316.44	0.4256	0.6524	316.24	0.4247	0.6517	315.88
−5.0000	0.1348	0.3671	177.9459	**0.1342**	**0.3663**	**177.59**	0.1346	0.3670	177.8670
0.0000	0.0427	0.2066	100.1161	**0.0428**	**0.2060**	**99.9820**	0.0431	0.2076	100.5570
5.0000	0.0135	0.1161	56.2900	**0.0134**	**0.1160**	**56.2700**	0.0142	0.1192	57.7170
10.0000	**0.0043**	**0.0655**	**31.7300**	0.0043	0.0660	31.7480	0.0051	0.0715	34.5360
15.0000	**0.0014**	**0.0370**	**17.9396**	0.0014	0.0372	18.0000	0.0022	0.0473	22.7740
20.0000	**0.0004**	**0.0212**	**10.2635**	0.0005	0.0214	10.4000	0.0014	0.0369	17.7050

The bold signified the good results.

Table 8: SNR_{imp} results of the comparison of different filtering techniques (EEMD, CEEMDAN, and EWT).

SNR (dB)	EWT	EEMD	CEEMDAN
−10	−0.006	**−0.0049**	**0.0072**
−5	−0.006	**−0.0016**	−0.0016
0	−0.010	**−0.0063**	−0.0539
5	−0.009	**0.0002**	−0.2317
10	**−0.029**	−0.0543592	−0.8016
15	**−0.076**	−0.0945439	−2.2257
20	**−0.226**	−0.4888794	−5.0418

The bold signified the good results.

In Tables 6–8, the proposed method demonstrates noteworthy outcomes when compared to various widely utilized and recently published methods [26]. The adaptability showcased by this method enables a versatile approach to treating ECG noise contamination, leading to competitive performance. Furthermore, the proposed method allows for a lower level of processing complexity in comparison to the CEEMDAN and EEMD processes, leveraging their empirical approaches in the proposed treatment.

In summary, the results suggest that the proposed method exhibits promising performance, offering adaptability and competitive outcomes in managing ECG noise. In addition, the method introduces a favorable balance by achieving effective noise reduction comparable to CEEMDAN and EEMD while maintaining a lower processing complexity. This underscores its potential utility in practical applications where both performance and computational efficiency are critical considerations.

5. Conclusion

In this study, we introduce the empirical wavelet transform (EWT) method as a promising approach for denoising ECG signals. The denoising results obtained using the EWT method are compared and extensively discussed in relation to several conventional filters. The evaluation metrics, including the smallest PRD, MSE, and RMSE values, as well as high SMP_{imp} and SNR_{out}, demonstrate the superior signal reconstruction capabilities of the proposed method.

The effectiveness of the EWT approach is further highlighted by its successful performance in the presence of various disturbances commonly encountered in ECG signals, such as additive white Gaussian noise, muscular artifacts (MA), EMG, and PLI. The EWT exhibits strong noise reduction capabilities and demonstrates outstanding robustness. Overall, our findings suggest that the proposed approach excels in both visual assessment and quantitative measurements, delivering exceptional results in signal visualization and analysis.

In conclusion, our study presents the empirical wavelet transform (EWT) method as an effective solution for denoising ECG signals. The comparative analysis demonstrates its superiority over conventional filters, yielding improved signal reconstruction with minimized distortions. Moreover, the EWT showcases remarkable performance in handling diverse noise sources, making it a valuable tool for enhancing the visualization and quantitative measurements of ECG signals [42].

Data Availability

No data were used to support the study.

Conflicts of Interest

The authors declare that they have no conflicts of interest.

Authors' Contributions

S. Dlimi curated the data and corrected the grammatical English. S. Elouaham and A. Dliou conceptualised the study and developed the methodology. S. Elouaham, A. Dliou, and W. Jenkal performed the formal analysis. S. Elouaham, M. Louzazni, and H. Zougagh investigated the study. H. Zougagh and S. Dlimi curated the data and wrote and prepared the original draft of the study. S. Elouaham, A. Dliou, W. Jenkal, M. Louzazni, H. Zougagh, and S. Dlimi wrote, reviewed, and edited the manuscript. S. Elouaham visualized and supervised the study.

References

[1] R. John, U. Tedrow, and B. Koplan, "Ventricular arrhythmias and sudden cardiac death," *Lancet*, vol. 380, p. 1520, 2012.

[2] World Health Organization, *Noncommunicable Diseases Country Profiles 2018*, World Health Organization, Geneva, Switzerland, 2018.

[3] M. A. Awal, S. S. Mostafa, M. Ahmad, and M. A. Rashid, "An adaptive level dependent wavelet thresholding for ECG denoising," *Biocybernetics and Biomedical Engineering*, vol. 34, no. 4, pp. 238–249, 2014.

[4] L. D. Sharma and R. K. Sunkaria, "Novel T-wave detection technique with minimal processing and RR-interval based enhanced efficiency," *Cardiovascular Engineering and Technology*, vol. 10, no. 2, pp. 367–379, 2019.

[5] L. D. Sharma and R. K. Sunkaria, "Detection and delineation of the enigmatic U-wave in an electrocardiogram," *International Journal of Information Technology*, vol. 13, no. 6, pp. 2525–2532, 2021.

[6] J. Rahul, M. Sora, and L. D. Sharma, "Exploratory data analysis based efficient QRS-complex detection technique with minimal computational load," *Physical and Engineering Sciences in Medicine*, vol. 43, no. 3, pp. 1049–1067, 2020.

[7] J. Rahul and L. D. Sharma, "Automatic cardiac arrhythmia classification based on hybrid 1-D CNN and Bi-LSTM model," *Biocybernetics and Biomedical Engineering*, vol. 42, pp. 312–324, 2022.

[8] S. Elouaham, A. Dliou, N. Elkamoun et al., "Denoising electromyogram and electroencephalogram signals using improved complete ensemble empirical mode decomposition with adaptive noise," *Indonesian Journal of Electrical Engineering and Computer Science*, vol. 23, no. 2, p. 829, 2021.

[9] M. B. Hossain, S. K. Bashar, J. Lazaro, N. Reljin, Y. Noh, and K. H. Chon, "A robust ECG denoising technique using variable frequency complex demodulation," *Computer Methods and Programs in Biomedicine*, vol. 200, 2021.

[10] S. Elouaham, R. Latif, B. Nassiri, A. Dliou, M. Laaboubi, and F. Maoulainine, "Analysis Electroencephalogram signals using ANFIS and Periodogram techniques," *International Review on Computers and Software*, vol. 8, no. 12, pp. 2959–2966, 2013.

[11] A. Dliou, S. Elouaham, R. Latif, M. Laaboubi, H. Zougagh, and A. Saddik, "Denoising ventricular tachyarrhythmia signal," in *Proceedings of the 2018 9th International Symposium on Signal, Image, Video, and Communications (ISIVC)*, pp. 124–128, Rabat, Morocco, November 2018.

[12] S. elouaham, A. Dliou, M. Laaboubi, R. Latif, N. Elkamoun, and H. Zougagh, "Filtering and analyzing normal and abnormal electromyogram signals," *Indonesian Journal of Electrical Engineering and Computer Science*, vol. 20, no. 1, pp. 176–184, 2020.

[13] S. Pal and M. Mitra, "Empirical mode decomposition-based ECG enhancement and QRS detection," *Computers in Biology and Medicine*, vol. 42, no. 1, pp. 83–92, 2012.

[14] M. A. Kabir and C. Shahnaz, "Denoising of ECG signals based on noise reduction algorithms in EMD and wavelet domains," *Biomedical Signal Processing and Control*, vol. 7, no. 5, pp. 481–489, 2012.

[15] M. Blanco-Velasco, B. Weng, and K. E. Barner, "ECG signal denoising and baseline wander correction based on the empirical mode decomposition," *Computers in Biology and Medicine*, vol. 38, no. 1, pp. 1–13, 2008.

[16] M. Rakshit and S. Das, "An efficient ECG denoising methodology using empirical mode decomposition and adaptive switching mean filter," *Biomedical Signal Processing and Control*, vol. 40, pp. 140–148, 2018.

[17] M. A. Kabir and C. Shahnaz, "Denoising of ECG signals based on noise reduction algorithms in EMD and wavelet domains," *Biomedical Signal Processing and Control*, vol. 7, no. 5, pp. 481–489, 2012.

[18] W. Jenkal, R. Latif, A. Toumanari, A. Dliou, O. El B'charri, and F. M. R. Maoulainine, "An efficient algorithm of ECG signal denoising using the adaptive dual threshold filter and the discrete wavelet transform," *Biocybernetics and Biomedical Engineering*, vol. 36, no. 3, pp. 499–508, 2016.

[19] B. N. Singh and A. K. Tiwari, "Optimal selection of wavelet basis function applied to ECG signal denoising," *Digital Signal Processing*, vol. 16, no. 3, pp. 275–287, 2006.

[20] M. A. Awal, S. S. Mostafa, M. Ahmad, and M. A. Rashid, "An adaptive level dependent wavelet thresholding for ECG denoising," *Biocybernetics and Biomedical Engineering*, vol. 34, no. 4, pp. 238–249, 2014.

[21] G. Lu, J. S. Brittain, P. Holland et al., "Removing ECG noise from surface EMG signals using adaptive filtering," *Neuroscience Letters*, vol. 462, no. 1, pp. 14–19, 2009.

[22] C. Marque, C. Bisch, R. Dantas, S. Elayoubi, V. Brosse, and C. Pérot, "Adaptive filtering for ECG rejection from surface EMG recordings," *Journal of Electromyography and Kinesiology*, vol. 15, no. 3, pp. 310–315, 2005.

[23] R. Sameni, M. B. Shamsollahi, C. Jutten, and G. D. Clifford, "A nonlinear Bayesian filtering framework for ECG Denoising," *IEEE Transactions on Biomedical Engineering*, vol. 54, no. 12, pp. 2172–2185, 2007.

[24] M. Br and S. Mr, "ECG denoising using wiener filter and kalman filter," *Procedia Computer Science*, vol. 171, pp. 273–281, 2020.

[25] J. Wang, Y. Ye, Y. Gao, S. Qian, and X. Gao, "Fractional compound integral with application to ECG signal denoising," *Circuits, Systems, and Signal Processing*, vol. 34, no. 6, pp. 1915–1930, 2015.

[26] A. Bajaj, S. Kumar, and Biomed, "A robust approach to denoise ECG signals based on fractional Stockwell transform," *Biomedical Signal Processing and Control*, vol. 62, 2020.

[27] S. Poungponsri and X. H. Yu, "An adaptive filtering approach for electrocardiogram (ECG) signal noise reduction using neural networks," *Neurocomputing*, vol. 117, pp. 206–213, 2013.

[28] M. R. Mohebbian, M. W. Alam, K. A. Wahid, and A. Dinh, "Single channel high noise level ECG deconvolution using optimized blind adaptive filtering and fixed point convolution kernel compensation," *Biomedical Signal Processing and Control*, vol. 57, 2020.

[29] G. Huang, L. Xu, Q. L. Chen, and M. R. Wang, "Image denoising using a fractional integral," in *Proceedings of the IEEE International Conference on Computer Science and Automation Engineering*, pp. 107–112, Zhangjiajie, China, May 2012.

[30] J. Gilles, "Empirical wavelet transform," *IEEE Transactions on Signal Processing*, vol. 61, no. 16, pp. 3999–4010, 2013.

[31] M. Sarkar, P. R. Sarkar, U. Mondal, and D. Nandi, "Empirical wavelet transform-based fog removal via dark channel prior," *IET Image Processing*, vol. 14, no. 6, pp. 1170–1179, 2020.

[32] H. Cao, F. Fan, K. Zhou, and Z. He, "Wheel-bearing fault diagnosis of trains using empirical wavelet transform," *Measurement*, vol. 82, pp. 439–449, 2016.

[33] Q. Zhang, J. Ding, and W. Zhao, "An adaptive boundary determination method for empirical wavelet transform and its application in wheelset-bearing fault detection in high-speed trains," *Measurement*, vol. 171, 2021.

[34] H. Yu, H. Li, and Y. Li, "Vibration signal fusion using improved empirical wavelet transform and variance contribution rate for weak fault detection of hydraulic pumps," *ISA Transactions*, vol. 107, pp. 385–401, 2020.

[35] Y. Liu, D. Yuan, Z. Gong, T. Jin, and M. A. Mohamed, "Adaptive spectral trend-based optimized EWT for monitoring the parameters of multiple power quality disturbances," *International Journal of Electrical Power & Energy Systems*, vol. 146, 2023.

[36] K. El Khadiri, S. Elouaham, B. Nassiri et al., "A comparison of the denoising performance using capon time-frequency and empirical wavelet transform applied on biomedical signal," *International Journal on Engineering Applications (IREA)*, vol. 11, no. 5, pp. 358–365, 2023.

[37] S. Elouaham, B. Nassiri, A. Dliou et al., "Combination time-frequency and empirical wavelet transform methods for removal of composite noise in EMG signals," *TELKOMNIKA (Telecommunication Computing Electronics and Control)*, vol. 21, no. 6, pp. 1373–1381, 2023.

[38] PhysioBank, "PhysioBank ATM," 2020, https://archive.physionet.org/cgi-bin/atm/ATM.

[39] G. B. Moody and R. G. Mark, "The impact of the MIT-BIH arrhythmia database," *IEEE Engineering in Medicine and Biology Magazine*, vol. 20, no. 3, pp. 45–50, 2001.

[40] G. B. Moody, W. E. Muldrow, and R. G. Mark, "A noise stress test for Arrhythmia detectors," *Computers in Cardiology*, vol. 11, no. 1, pp. 381–384, 1984.

[41] A. Dliou, S. Elouaham, R. Latif, and M. Laaboubi, "Combination of the CEEM decomposition with adaptive noise and periodogram technique for ECG signals analysis," *Chapter in Practical Applications of Electrocardiogram*, Intechopen, London, UK, 2019.

[42] S. Elouaham, A. Dliou, B. Nassiri, and H. Zougagh, "Combination method for denoising EMG signals using EWT and EMD techniques," in *Proceedings of the 2023 IEEE International Conference on Advances in Data-Driven Analytics and Intelligent Systems (ADACIS)*, pp. 1–6, Marrakesh, Morocco, November 2023.